Research on Engineering Structures & Materials
www.jresm.org
Research Group

Research Article

Thermo-physical and mechanical characterization of an eco-friendly insulating brick incorporating dune sand and crushed desert rose aggregates

Abdelaziz Logbi [1,2], Laid Bedadi [1,2], Tahar Zerig [3], Mohammed Mani [1,2], Tarek Djedid [*,1,4]

[1]*Department of Hydraulic and Civil Engineering, Faculty of Technology, University of El Oued, 39000, Algeria*
[2]*Unit for the development of renewable energy in arid areas (UDERZA), Algeria*
[3]*Laboratory LGCH, University 8 May 1945 Guelma, Algeria*
[4]*Laboratory of exploitation and valorization of Saharan energy resources "LEVRES", faculty of exact sciences, University of El Oued, 39000, Algeria*

Article Info

Article History:

Received 05 Sep 2026
Accepted 19 Oct 2026

Keywords:

Desert rose;
Dune sand;
Cement-based composites;
Thermal insulation;
Sustainable construction;
Low-carbon building materials;
Heritage restoration

Abstract

This paper contributes to the development of an eco-friendly composite cementitious material using local resources from southeastern Algeria, a Saharian region characterized by an arid climate with scorching summers and severe winters. To address these climatic and environmental challenges, the conventionally used alluvial sand (AS) and quarry gravel were substituted with Saharan dune sand (DS) and crushed desert rose (CDR), a local stone historically utilized in traditional Saharan construction. The desert rose was crushed and graded into two particle sizes (3/8 mm and 8/15 mm), while the dune sand was incorporated into the alluvial sand at varying substitution rates (0%, 10%, 20%, 40%, and 50%). A concrete mix design was developed based on these two aggregates and used to manufacture solid bricks measuring (4x10x16 cm). Experimental results indicate that the optimal formulation, consisting of 40% dune sand (DS) combined with crushed desert rose (CDR), exhibited highly promising physical, mechanical, and thermal properties. Consequently, this sustainable material offers a superior alternative to traditional raw materials. Furthermore, it provides a resilient solution to climate change compared to modern industrial materials, thereby preserving local thermal comfort as well as the unique architectural and historical heritage of the region.

© 2026 MIM Research Group. All rights reserved.

1. Introduction

The building sector is among the largest consumers of energy worldwide and is responsible for a substantial share of global greenhouse gas emissions. In hot-arid regions, the increasing frequency and intensity of heat waves have further intensified the demand for electricity, primarily because of the widespread use of air-conditioning systems. Algeria has recently experienced this challenge. During the summers of 2024, 2025, and 2026, the country recorded unprecedented electricity demand, reaching 21,378 MW, which resulted in large-scale power outages affecting several provinces in eastern and southeastern Algeria [1]. In response, the Algerian government has reinforced its commitment to sustainable construction by promoting energy-efficient buildings and encouraging the use of locally available, environmentally friendly construction materials, particularly in the hot desert regions of southern Algeria [2]. Recent studies have increasingly emphasized the importance of replacing conventional construction materials with low-carbon, bio-

*Corresponding author: tarek-djedid@univ-eloued.dz
[a]orcid.org/0000-0001-5263-8901; [b]orcid.org/0000-0002-0284-1204; [c]orcid.org/0000-0002-6713-4666;
[d]orcid.org/0000-0003-0069-3567; [e]orcid.org/0000-0002-1249-156X
DOI: http://dx.doi.org/10.17515/resm2026-2299ma0905rs

based, and locally available alternatives to reduce the environmental footprint of the building sector. Such materials generally exhibit lower embodied energy, improved thermal performance, and enhanced circularity, making them promising candidates for sustainable construction in hot and arid climates [3-10]. Despite these advances, relatively limited attention has been devoted to the valorization of desert geological resources as aggregates in cement-based composites, particularly for applications combining sustainable construction and heritage conservation. Southern Algeria is characterized by a hyper-arid climate, where summer temperatures frequently approach 50 °C, whereas winter temperatures may fall to nearly 0 °C. Such severe thermal fluctuations require building envelopes with high thermal performance to ensure indoor comfort while minimizing cooling and heating energy consumption [11-13]. For centuries, vernacular architecture successfully addressed these climatic constraints through the use of locally sourced materials. Traditional buildings were constructed using fired local gypsum mixed with dune sand and natural desert rose stone (DR), often reinforced with date-palm fibers [14,15]. Combined with passive architectural elements such as domes and vaults, these materials provided excellent thermal and acoustic insulation while maintaining satisfactory indoor comfort under extreme climatic conditions [16-20]. In addition to their thermal efficiency, these materials exhibited a remarkably low environmental impact because they required limited processing energy, generated very low CO_2 emissions, and enabled the valorization of agricultural residues from date palms as fuel for traditional gypsum kilns [21-23]. Despite these advantages, traditional construction materials have progressively been replaced by industrial products such as reinforced concrete, fired clay bricks, synthetic gypsum, and crushed quarry aggregates. Although these materials satisfy modern engineering requirements, their production is associated with high embodied energy and significant greenhouse gas emissions, resulting in a considerably larger environmental footprint [24, 25]. Consequently, there is increasing interest in developing sustainable construction materials based on abundant local resources capable of reducing both environmental impacts and operational energy consumption. An additional challenge concerns the conservation of historical buildings in southern Algeria. Most of these structures were originally built using traditional gypsum, dune sand, and desert rose stone, materials that have become increasingly scarce or difficult to exploit. Furthermore, traditional gypsum exhibits poor resistance to moisture, limiting its durability under certain environmental conditions and complicating restoration interventions (Figure 1). Therefore, developing an alternative material capable of reproducing the beneficial properties of traditional composites while improving durability represents an important scientific and practical challenge.

Several studies have investigated the incorporation of natural aggregates, mineral additives, and fibers into gypsum- or dune-sand-based matrices to enhance their mechanical, thermal, and durability performance [5, 16, 17, 18, 26-28]. Zerig et al. demonstrated that incorporating dune sand in equal proportions markedly enhanced the mechanical and physical performance of mortar. These findings highlight the potential of dune sand as a viable and efficient constituent for the development of high-performance mortar, particularly in regions where this abundant local resource is readily available [29-32]. Nevertheless, research on cement-based composites incorporating crushed desert rose aggregates in combination with dune sand remains extremely limited. Recent reviews have emphasized the need to explore alternative locally available aggregates capable of reducing the environmental footprint of cementitious materials while maintaining satisfactory engineering performance [33-35]. Despite growing interest in local construction materials, the combined utilization of crushed desert rose (CDR) and dune sand in cementitious matrices remains unexplored. This represents a critical research gap, particularly regarding their physical-chemical compatibility, granular packing optimization, and thermal-mechanical trade-offs. Although gypsum-rich aggregates like CDR typically compromise mechanical strength and increase water absorption, this study addresses these limitations by pairing two distinct CDR particle-size fractions (3–8 mm and 8–15 mm) with progressive dune-sand substitution levels (0–50 wt.%). Motivated by the urgent need for low-carbon building solutions in arid regions, this work provides a systematic evaluation of the resulting composite bricks. The objective is to identify an optimal formulation using exclusively local resources that satisfies modern building energy standards while ensuring full material compatibility for heritage restoration.



Fig. 1. (a) Traditional construction technique using desert rose (DR) stones and locally produced gypsum. (b and c) Photograph of a deteriorated traditional house prior to restoration. (d) Historic alleyway in the old city following restoration and rehabilitation

2. Materials Used

2.1 Cement

The binder used in this investigation was an ordinary Portland cement (CEM II/B-L 42.5 N) conforming to the requirements of the Algerian standard NA 442-2013 and the European standard EN 196-1. The cement's chemical composition, mineralogical phases, and principal physical properties are presented in Table 1.

Table 1. Chemical composition, mineralogical phases, and main physical properties of the cement used

Chemical composition					Mineralogical composition	
Element	MgO	SO_3	Chloride content	LOI	% C_3S	% C_3A
%	1.2 ~ 2.2	2~3	0.02 - 0.05	8 ~ 12	57 ~ 63	6.5~ 8.5
Physical characteristics						
Fineness (specific surface Blaine; SSB) (cm^2/g)	Apparent volumetric weight (g/cm^3)	Absolute volumetric weight (g/cm^3)	Initial setting time (min)	Final setting time (min)	Normal consistency (%)	28-day shrinkage	Expansion (mm)
3700-5200	1,014	3,082	120-180	180-280	24.5-28.5	< 1000μm/m	≤ 3mm

2.2 Desert Rose Stone

The desert rose is a sedimentary rock primarily composed of gypsum crystals (calcium sulfate dihydrate, $CaSO_4$-$2H_2O$) containing inclusions of desert sand. It forms in arid environments through the evaporation of groundwater that has infiltrated sandy sediments. Its characteristic rosette-like morphology, which resembles the petals of a rose, gives rise to its name. This distinctive crystal habit typically develops under dry, sandy conditions during gypsum crystallization [36].

The sand rose used in this study was collected from the Souf region in southeastern Algeria. It is distinguished by its good thermal insulation properties, high mechanical strength and hardness, and relatively low porosity. Its physical and chemical characteristics are summarized in Table 2.

Table 2. Physical and chemical characterization of the different classes of crushed sand rose

Classes of gravel (CDR)	Apparent density (g/cm³)	Absolute density (g/cm³)	Water absorption coefficient (%)	Chemical composition
3/8 mm	1.045	2.38	9.91	calcium sulfate dihydrate, $CaSO_4$,$2H_2O$
8/15 mm	1.097	2.38	15.38	

The desert rose stone was crushed and sieved into two aggregate size fractions (3–8 mm and 8–15 mm). These size ranges were selected because they are widely used in conventional concrete mixtures and are suitable for the dimensions of the bricks produced in this study (40 × 100 × 160 mm³). The corresponding particle-size distributions are shown in Figure 2.

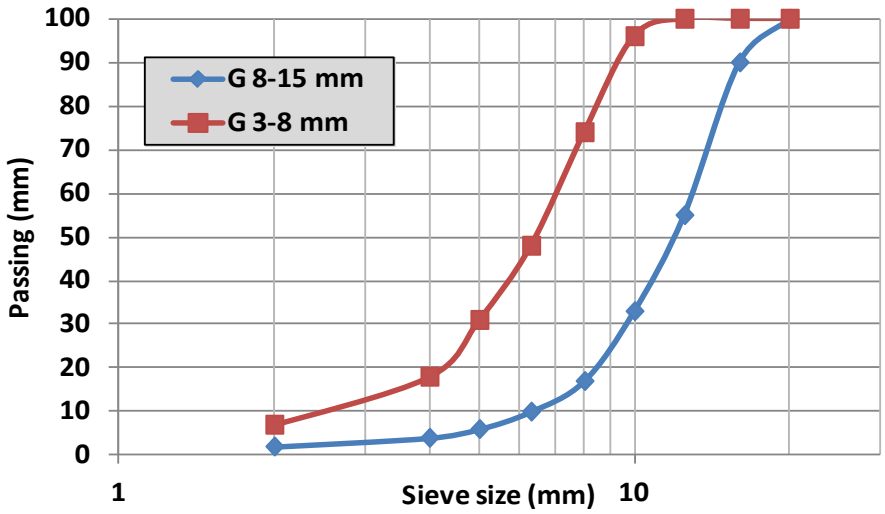


Fig. 2. Particle size distributions of the different crushed desert rose aggregate fractions

2.3 Dune Sand

Dune sand is a naturally occurring Aeolian material formed through the gradual weathering and erosion of rocks by wind, rainfall, and other environmental agents. It is characterized by its very fine particle size (0–0.63 mm), high cleanliness, and predominantly siliceous composition (Figure 3 and 4) [37]. Owing to its wide availability in southern Algeria and its favorable physical and chemical properties, dune sand has attracted increasing attention as an alternative aggregate in concrete, mortar, and road construction applications [28, 35, 38, 39].

In the present study, dune sand was collected from the Oued Souf region in southeastern Algeria. Chemical analysis revealed a high silica (SiO2) content confirming its predominantly siliceous nature, as illustrated in (Figure 3 and 4) and (Table 3). Its particle size analysis is shown in Figure 4.c.

Table 3. Chemical and physical characteristics of dune sand (DS) and alluvial sand (AS) used

	Content of silica (SiO_2)	Finesse module (NF P 18–540-EN12620)	Apparent volumetric weight (g/cm^3)	Absolute volumetric weight (g/cm^3)	Sand equivalent (NF P18- 2598)
Dune Sand (DS)	80	1,01	1,77	2,67	88
Alluvial Sand (AS)	80~90%	1,98	1,83	2,68	70

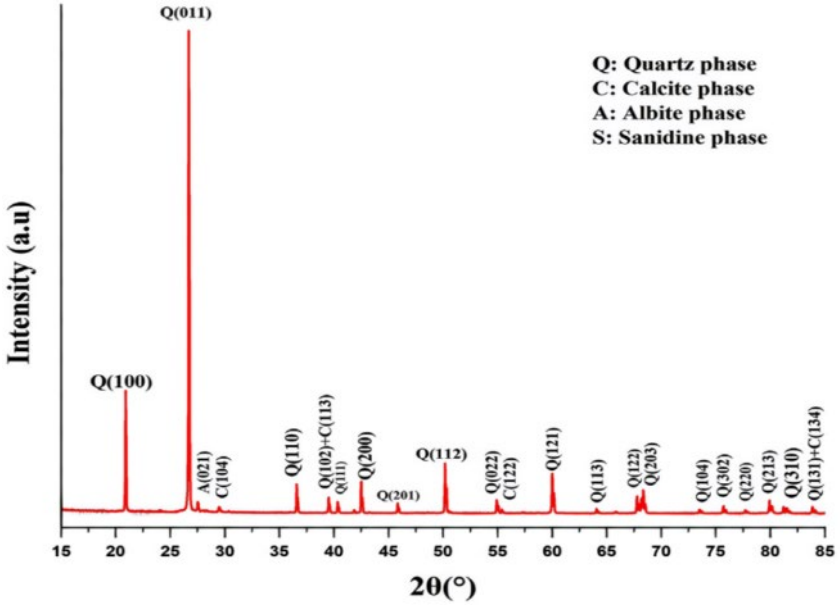


Fig. 3. The X-Ray Diffraction pattern of the dune sand used [37]

2.4 Alluvial Sand

The natural sand used in the preparation of the different mixtures was alluvial sand (AS) collected from the Djamaa region (southeastern Algeria). This sand was selected from several locally available sources based on its favorable physical characteristics and particle-size distribution, making it suitable for the intended applications. Its main physical properties and grading curve are presented in Figure 4.c and Table 3

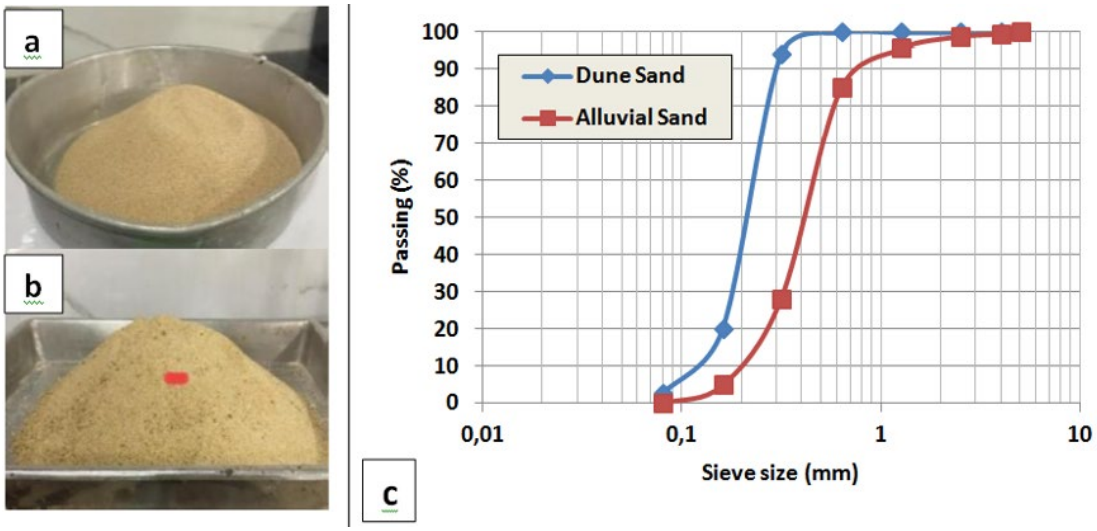


Fig. 4. (a) Dune sand (DS) used. (b) Alluvial sand (AS) used. and (c) Particle size analysis of dune sand (DS) and alluvial sand (AS) used

3. Methods and Testing Procedures

3.1 Experimental Protocol

The different stages of the experimental program are described below.

- Stage 1: Optimization of the dune sand incorporation rate

A reference mortar with a standard composition was prepared using one part cement, three parts sand (by weight), and a water-to-cement ratio (W/C) of 0.5; (NF EN 196-1). To evaluate the effect of dune sand on the mechanical performance of the mortar, dune sand was used as a partial replacement for the alluvial sand at replacement levels of 0, 10, 20, 30, 40, and 50 wt.%, (Table 4), these percentages were selected based on a previous study by M. Mani et al., [40]. The objective of this first stage was to determine the optimum dune sand replacement level based on the mechanical strength of the resulting mortars. The physical and mechanical performances of the different mixtures were evaluated using prismatic specimens measuring 40 × 40 × 160 mm.

Table 4. Weight composition of the different mortars studied

Weight composition of the different mortars studied				
Mixture	Alluvial sand (g)	Dune sand (g)	Cement (g)	Water (ml)
Control mortar CM	1350	0	450	225
Mortar M10	1215	135	450	225
Mortar M20	1080	270	450	225
Mortar M30	945	405	450	225
Mortar M40	810	540	450	225
Mortar M50	675	675	450	225

- Stage 2: Formulation of concrete incorporating crushed desert rose aggregates

Based on the optimum mortar composition identified in the first stage, crushed desert rose stone (CDR) was used as the coarse aggregate. Three concrete mixtures were prepared by varying the proportions of two aggregate size fractions (3–8 mm and 8–15 mm), while maintaining a constant water-to-cement ratio (W/C = 0.5), as summarized in Table 5. To reflect conventional brick manufacturing practice, the concrete was designed using a weight-based mix proportion of 1:2:3 (cement: sand (AS+DS): crushed desert rose aggregate (CDR)), while maintaining a constant water-to-cement ratio (W/C) of 0.50. This practical and straightforward mix design was intentionally selected to facilitate industrial implementation and to demonstrate the feasibility of producing sustainable bricks using locally available materials without modifying conventional manufacturing practices. The mixing water content was carefully adjusted to ensure adequate workability without affecting the properties investigated. To minimize water absorption by the aggregates and maintain the consistency of the fresh mixtures, the crushed desert rose (CDR) aggregates were pre-soaked to a saturated condition before mixing. The physical and mechanical properties of the different mixtures were evaluated using (100 × 100 × 100 mm) cubic specimens.

- Stage 3: Brick manufacturing and physical, mechanical, and thermal characterization

Following the experimental investigation, the optimum mixture was selected for the manufacture of solid bricks with dimensions equivalent to those of commercially available units (160 × 100 × 40 mm). The thermal performance of the developed bricks was then experimentally compared with that of conventional solid bricks available on the local market (Figure 5). A summary of the investigated mixtures and the notation adopted throughout this study is provided in Table 5.

3.2 Crushing and Screening of Desert Roses Stone

Following extraction, the sand roses were thoroughly cleaned and washed to remove dust and other undesirable impurities. They were then crushed and sieved to produce three aggregate size fractions (3–8 mm and 8–15 mm) in accordance with the requirements of NF EN 933-1 [41]. The different stages of the crushing and screening process are illustrated in Figure 6.

Table 5. Mix proportions of crushed desert rose (CDR) aggregate and dune sand (DS) fractions used in the concrete mixtures

Concrete Mixture	Mix proportion of 1:2:3 (cement: sand (AS+DS): Crushed desert rose aggregate (CDR))				
	weight-based dosage of different classes of aggregate (CDR)		weight-based dosage of sand		Water-to-cement ratio (W/C)
	CDR 3-8 mm	CDR 8-15 mm	Dune sand (DS)	Alluvial sand (AS)	
Mixe C :3-8	100%	0%	40%	60%	0,5
Mixe C :8-15	0%	100%	40%	60%	0,5
Mixe C :3-8 and 8-15	50%	50%	40%	60%	0,5
Batch composition by weight for three (100 x 100 x 100 mm³) cubic specimens					
Mixture	Cement (g)	CDR 3-8 mm (g)	CDR 8-15 mm (g)	Dune sand (DS) (g)	Alluvial sand (AS) (g)	Water (ml)
Mixe C :3-8	1100	3300	0	880	1320	550
Mixe C :8-15	1100	0	3300	880	1320	550
Mixe C :3-8 and 8-15	1100	1650	1650	880	1320	550
Batch composition by weight for three solid brick specimens (40 × 100 × 160 mm³)						
Mixture	Cement (g)	CDR 3-8 mm (g)	CDR 8-15 mm (g)	Dune sand (DS) (g)	Alluvial sand (AS) (g)	Water (ml)
Mixe C :3-8	750	2250	0	600	900	375
Mixe C :8-15	750	0	2250	600	900	375
Mixe C :3-8 and 8-15	750	1125	1125	600	900	375



Fig. 5. Representative specimens used throughout the experimental program: (a) mortar prism (40 × 40 × 160 mm³); (b) concrete cube (100 × 100 × 100 mm³); and (c) manufactured solid brick (40 × 100 × 160 mm³)

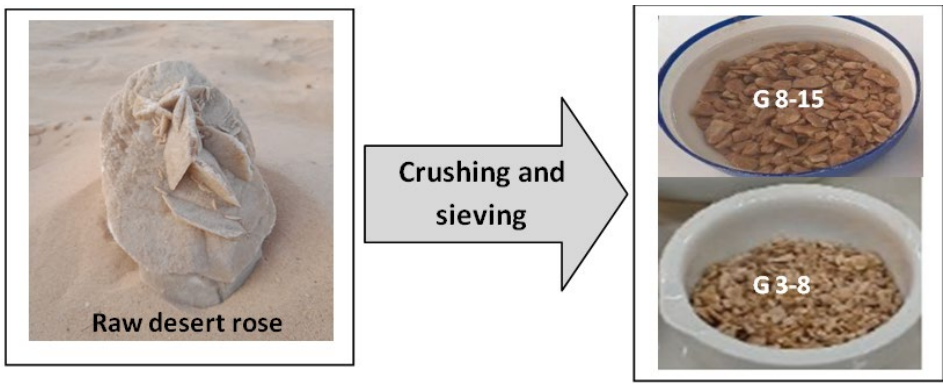


Fig. 6. Preparation process of crushed desert rose aggregates (CDR): from raw desert rose stone to sieved fractions (G 8–15 mm and G 3–8 mm)

3.3 Test Procedures

The experimental program included the following physical and mechanical characterization tests.

3.3.1 Physical and Mechanical Characterization

Water absorption through full immersion (WA) was measured according to NBN B 15-215 [42]. The specimens were completely immersed in fresh water until full saturation (Figure 7.a), yielding the saturated mass (Msat), and were subsequently dried to a constant mass (Mdry). The water absorption by immersion (WA) was calculated using Equation (1):

$$Water\ Absorption\ (\%) = \frac{M_{sat} - M_{dry}}{M_{dry}} x\ 100\% \quad (1)$$

Water capillary absorption (CA) was determined in accordance with EN 1015-18 [43]. To ensure one-dimensional water flow, the lateral faces of the specimens were sealed with epoxy resin (Figure 7.b), while the bottom surface was placed in contact with water maintained at a constant level of 4 mm. The sorptivity coefficient (S) was calculated after 72 hours of immersion using Equation (2):

$$\frac{Q}{A} = S.\sqrt{t} \quad (2)$$

where Q is the cumulative volume of absorbed water, A is the exposed surface area, t is the elapsed time (t=72h).

Ultrasonic pulse velocity (UPV) tests were carried out in accordance with BS EN 12504-4 [44]. to evaluate the quality and internal integrity of the specimens. Mechanical strength tests: Flexural and compressive strengths were determined according to EN 196-1 [45]. Flexural strength was measured using a three-point bending test (Figure 8.). For the mortar mixtures, the two halves of each prismatic specimen obtained after the flexural strength test were subsequently used to determine the compressive strength (Figure 8.b). In contrast, for the concrete mixtures incorporating dune sand and crushed desert rose (CDR) aggregates, the compressive strength test was performed directly on hardened cubic specimens (Figure 8.c).

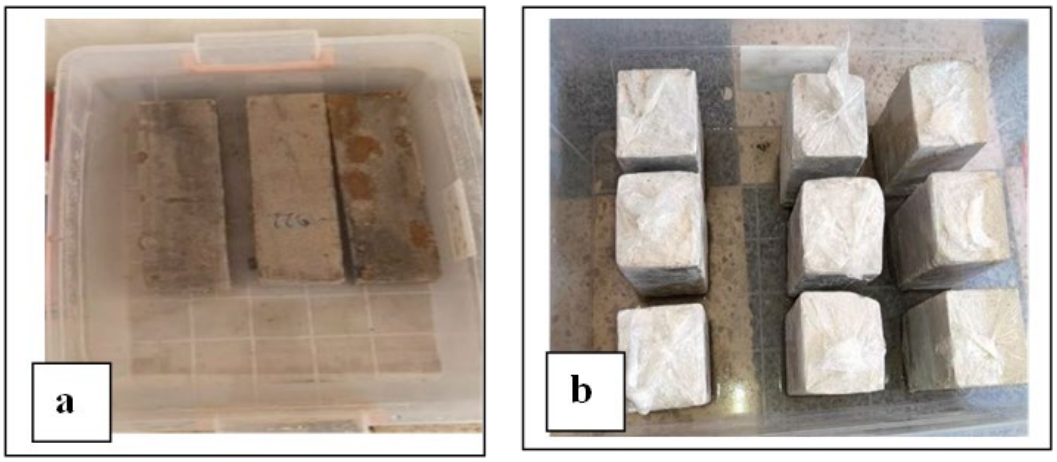


Fig. 7. Water absorption tests: (a) Water absorption through full immersion test; (b) Capillary water absorption test

3.3.2 Thermal Characterization

Thermal response test. The thermal behavior of the specimens was evaluated by monitoring heat propagation through the material. The test consisted of measuring the temperature difference between the surface directly exposed to a heat source and the opposite surface, as illustrated in Figure 9. The experimental procedure was as follows:

- The specimens were placed on a heated plate to ensure continuous heat transfer through the material.

- After a heating phase (150 min), the specimens were removed from the hot plate and allowed to cool under ambient laboratory conditions (approximately 20 °C). for another 150 min.
- During the heating and cooling phases, the temperatures of the exposed (internal) and unexposed (external) faces (Tint and Text) were measured every 30 minutes until thermal equilibrium was reached.
- The rate of heat dissipation was evaluated from the evolution of the temperature difference (ΔT=Tint-Text) between the two faces.

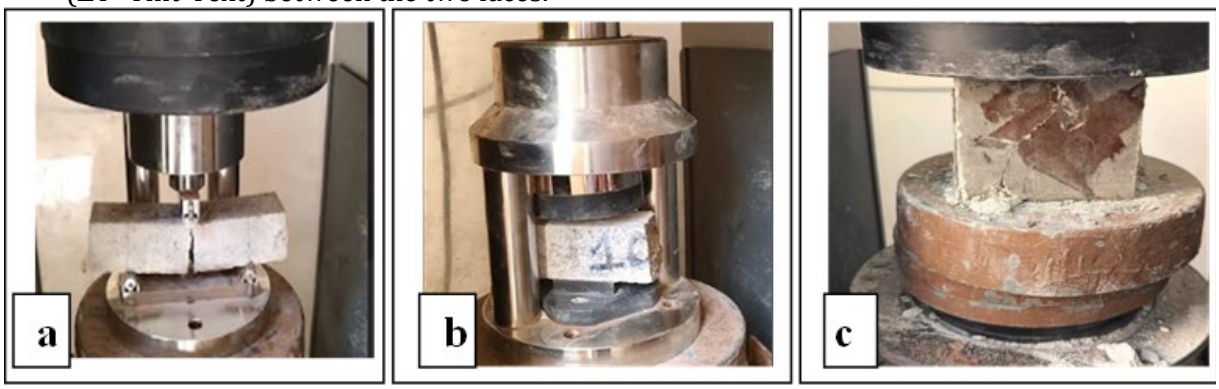


Fig. 8. Mechanical strength tests: (a) flexural strength test on mortar specimens; (b) compressive strength test on mortar specimens; (c) compressive strength test on concrete specimens

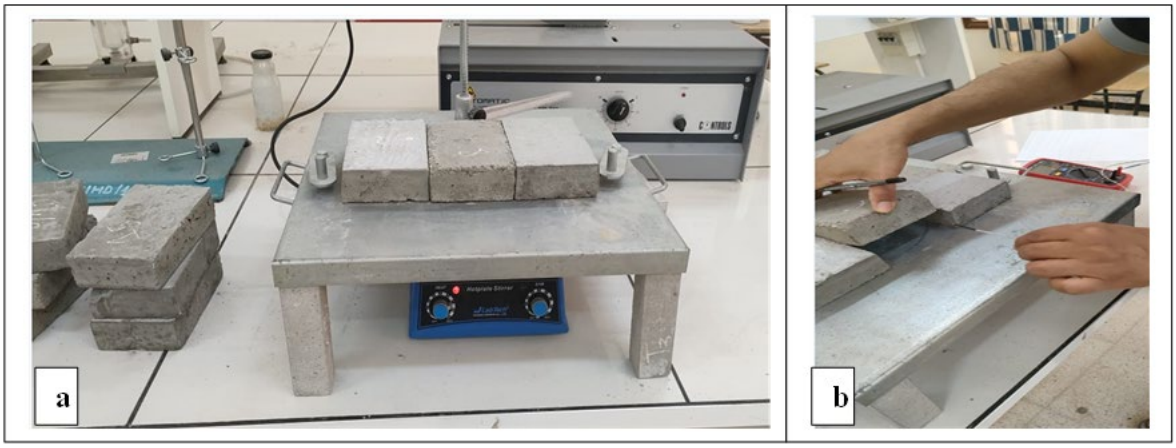


Fig. 9. Thermal characterization test, (a) heating of bricks; and (b) temperature measurements

4. Results and Discussion

4.1 Mechanical Properties

4.1.1 Optimization of the Dune Sand Incorporation Rate

A preliminary experimental program was conducted to determine the optimum incorporation rate of dune sand as a partial replacement for alluvial sand. The primary objective was to maximize the utilization of this locally abundant resource in cement-based construction materials while maintaining satisfactory mechanical performance. In our study, compressive strength was selected as the primary criterion for determining the optimum replacement level. As shown in Figure 10 and 11, the partial replacement of alluvial sand with dune sand did not adversely affect the mechanical performance up to a replacement level of 40%. In particular, the mixture containing 40% dune sand (M40) achieved a compressive strength of 20.5 MPa, which was very close to that of the control mortar (CM). This result indicates that, within the range investigated, a substantial proportion of alluvial sand can be replaced by dune sand without compromising the mechanical performance of the mortar. This observation is consistent with the findings reported by Mani et al. [40] and Fatema Ahmed et al. [26], who investigated the correction of dune-sand grading through blending with natural sand and reported satisfactory mechanical performance for mixtures

containing approximately 40% dune sand and 60% natural sand. A similar trend was observed for flexural strength (Figure 10). The maximum strength was achieved with a 10% dune sand content (M10), representing a 43% improvement over the control mortar (CM). This confirms the beneficial effect of dune sand in densifying the overall granular skeleton of the mortar by properly optimizing the particle size distribution of the alluvial sand. At a maximum substitution level of 40% (M40), the flexural strength remained higher than that of the control, showing a 21% increase. Beyond 40%, a drop in strength was observed, indicating a detrimental effect above this threshold. This loss in strength can be attributed to the extremely fine particle size of the dune sand, which increases the demand for binder and water. Similarly, the comprehensive review conducted by Jawad et al. concluded that dune sand can generally be incorporated into concrete at replacement levels of up to approximately 40% without significant adverse effects on strength and durability [28]. The authors further attributed the deterioration observed at higher replacement levels mainly to the excessive fineness and poor grading of dune sand.

More recent investigations have further demonstrated that the optimum replacement level is strongly dependent on the particle-size distribution, surface characteristics, treatment condition, and overall mix design. Hamada et al. [46], for example, reported that treated desert sand could be incorporated at levels as high as 50%, with the 50% mixture achieving the highest compressive strength in their experimental program. However, increasing the desert-sand content progressively reduced workability, while flexural and tensile strengths tended to decrease at higher replacement levels. These findings demonstrate that the optimum proportion of desert sand cannot be considered universal and must be determined according to the characteristics of the sand and the targeted properties of the composite material. More recently, Akhtar et al., in a systematic review of recycled and desert sand substitution, reported that moderate replacement levels generally provide more favorable mechanical performance, whereas higher replacement ratios can result in progressive reductions in strength and durability [35]. Their analysis also emphasized the potential of sustainable sands to reduce dependence on natural river sand and associated environmental impacts.

The satisfactory mechanical performance observed at a 40% replacement level in the present study can be partly attributed to the complementary particle-size distributions of the alluvial and dune sands. Because dune sand is significantly finer than conventional alluvial sand, its partial incorporation may allow the finer particles to occupy some of the interparticle voids within the coarser alluvial-sand skeleton. This filler or particle-packing effect can increase the compactness of the granular skeleton and reduce the volume of larger voids within the mixture. At moderate replacement levels, this beneficial effect may compensate for the less favorable characteristics associated with the high fineness and relatively uniform particle size of dune sand. Similar mechanisms have been reported in recent studies, where the appropriate incorporation of desert sand was associated with improved particle packing and, in some cases, a refinement of the pore structure.

However, when the dune-sand content exceeds an optimum level, the increasing proportion of very fine particles may progressively reduce the efficiency of the granular skeleton. This behavior was observed in the present study for M50, containing 50% dune sand, for which the compressive strength decreased to approximately 17 MPa, corresponding to a reduction of about 20% relative to the control mortar. This decrease can reasonably be associated with the excessive fineness of the dune sand, which increases the specific surface area of the solid particles and consequently the water demand of the mixture. If the available mixing water is insufficient to maintain adequate workability and particle dispersion, the resulting mixture may become less compact and more susceptible to the formation of voids. In addition, the relatively narrow particle-size distribution of dune sand may limit the development of an efficiently packed granular skeleton when its proportion becomes excessive. The resulting increase in porosity and/or reduction in the efficiency of cement-particle bonding can ultimately lead to a reduction in compressive strength. These mechanisms are consistent with the deterioration in mechanical performance reported for high desert-sand replacement ratios in the literature.

It is also worth noting that the optimum replacement level is not necessarily identical for all mechanical properties. For instance, Hamada et al. found that treated desert sand could increase compressive strength at a 50% replacement level, while flexural and tensile strengths showed a decreasing trend beyond 25% [46]. This finding highlights the importance of considering the specific characteristics of the dune sand and the target performance of the material when defining an optimum replacement ratio. Therefore, the 40% value identified in the present study should be regarded as the optimum level within the investigated experimental conditions, rather than as a universal optimum for all dune-sand-based cementitious materials.

Based on the experimental results obtained in the present study, a 40% dune-sand replacement level (M40) was therefore selected as the optimum incorporation rate among the mixtures investigated. This proportion represents a suitable compromise between maximizing the valorization of dune sand and maintaining adequate mechanical performance. Accordingly, a constant replacement level of 40% dune sand was adopted in all subsequent concrete mixtures incorporating crushed desert rose (CDR) aggregates. Maintaining a constant fine-aggregate composition allows the subsequent experimental investigation to focus specifically on the effect of the CDR aggregate gradation and size distribution, while minimizing the influence of variations in the fine-aggregate fraction. The selected formulation therefore provides a practical basis for developing a cement-based composite incorporating a substantial proportion of locally available mineral resources while maintaining satisfactory mechanical performance. From a sustainability perspective, this approach simultaneously contributes to the valorization of abundant desert resources and to the reduction of dependence on conventional alluvial or river sand, which is increasingly associated with environmental pressures arising from intensive extraction.

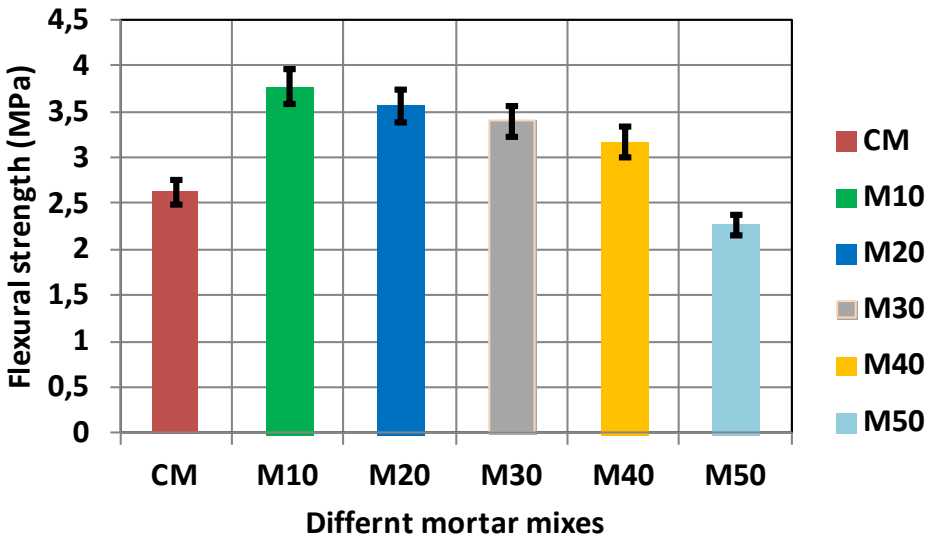


Fig. 10. Flexural strength of different mortar mixes

4.1.2 Effect of Crushed Desert Rose Aggregate Gradation on Compressive Strength

Following the optimization of the dune-sand replacement level, which was established at 40%, the experimental program was extended to investigate the mechanical performance of concrete mixtures incorporating both dune sand (DS) and crushed desert rose (CDR) aggregates. Three concrete formulations were selected based on the results of a recent experimental study previously conducted and published by the authors [24]. The selected formulations were designed to investigate the effect of CDR aggregate size distribution while maintaining the other mixture parameters constant. Accordingly, three aggregate configurations were considered: C:3–8, containing exclusively the 3–8 mm CDR fraction; C:8–15, containing exclusively the 8–15 mm fraction; and C:3–8/8–15, containing an equal proportion of the two size fractions. The detailed compositions of these mixtures are presented in Table 5.

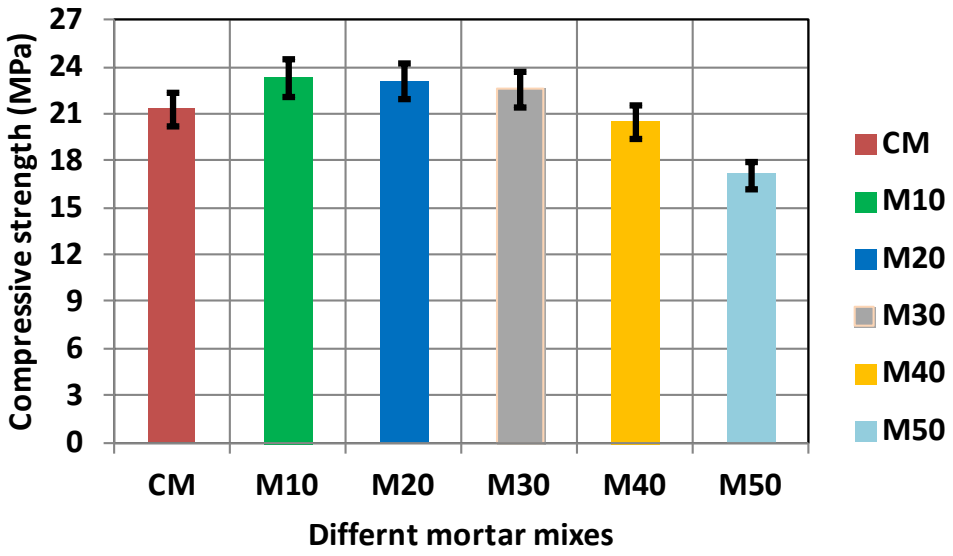


Fig. 11. Compressive strength of different mortar mixes

The results presented in Figure 12 show that all three mixtures developed satisfactory compressive strength, demonstrating the technical feasibility of incorporating CDR as a coarse aggregate in cement-based composite containing 40% dune sand. However, a clear difference was observed between the investigated gradations. The C:8–15 mixture exhibited the highest compressive strength, reaching approximately 20 MPa, which was very close to the compressive strength obtained for the reference M40 mortar. This result suggests that, under the experimental conditions adopted in this study, the exclusive use of the 8–15 mm CDR fraction provided a more favorable aggregate skeleton than the other investigated configurations.

The superior performance of the C8–15 mixture may be associated with the particle packing characteristics of the overall granular skeleton. In the present mixtures, the aggregate system consisted of alluvial sand, 40% dune sand, and CDR coarse aggregates. The relatively coarse 8–15 mm fraction may have provided a more favorable framework for the load-bearing skeleton, while the fine fractions supplied by the alluvial and dune sands occupied part of the interparticle voids. Such a combination can promote a more efficient distribution of particles across different size ranges and consequently reduce internal voids. The resulting increase in packing efficiency can contribute to improved stress transfer through the cementitious matrix and, ultimately, to higher compressive strength. Recent research has confirmed that aggregate size and grading can significantly influence the internal structure and mechanical response of concrete. Ukpata et al. [47], for instance, demonstrated that variations in aggregate size affect the performance of cement-based composites, emphasizing the importance of aggregate gradation in achieving an appropriate granular skeleton.

Therefore, the higher strength obtained with the C:8–15 mixture may not only result from differences in particle packing but could also be associated with differences in the aggregate–paste interfacial characteristics. In contrast, the mixtures incorporating the 3–8 mm CDR fraction, either alone or combined with the 8–15 mm fraction, exhibited lower compressive strengths. This behavior may be related to a less favorable packing configuration of the complete aggregate system. The addition of a relatively high proportion of the smaller CDR fraction may modify the balance between the coarse and fine particles and increase the total specific surface area of the aggregate phase. Consequently, a greater amount of cement paste may be required to adequately coat the particles and maintain efficient bonding. Under a constant water-to-cement ratio of 0.50, this effect may also influence the workability and internal compactness of the mixtures. Thus, the lower strength observed for C:3–8 and C:3–8/8–15 should be interpreted as the result of the combined effect of aggregate gradation, particle packing, surface area, and the intrinsic properties of CDR, rather than being attributed solely to aggregate size. Another factor that may explain the differences between the mixtures is the mechanical nature of the desert rose aggregate itself. Unlike conventional siliceous or silico-calcareous crushed aggregates commonly used in concrete, desert

rose is a relatively fragile evaporitic material with a gypsum-rich mineralogical nature. The crushing process may therefore generate particles with a more irregular and potentially weaker internal structure. The mechanical response of the resulting concrete is consequently governed by the intrinsic strength and stiffness of the CDR particles. This was confirmed by Dias et al. [34], who emphasized that the mechanical performance of concrete incorporating alternative aggregates is highly dependent on the nature of the aggregate. This consideration is particularly relevant to the present study, where CDR differs significantly from conventional aggregates in terms of mineralogical composition, particle morphology, and mechanical behavior. An interesting aspect of the present results is that the C:8–15 mixture achieved a compressive strength of approximately 20 MPa despite incorporating a relatively unconventional aggregate and 40% dune sand. This finding demonstrates that the use of locally available desert resources does not necessarily result in a significant loss of mechanical performance when their proportions and particle sizes are appropriately selected. Instead, the results suggest that the combination of dune sand with a suitable CDR size fraction can produce a mechanically viable cement-based composite. This observation is particularly relevant for the intended application of the material in solid brick production, where very high structural concrete strength is not necessarily required, whereas adequate compressive strength, thermal performance, local availability, and environmental compatibility are important design criteria.

It should also be emphasized that the C:8–15 formulation was identified as the best-performing mixture within the experimental configurations investigated. Overall, the results indicate that aggregate gradation plays a decisive role in the mechanical performance of the proposed DS–CDR composite. Among the three configurations investigated, the C:8–15 mixture provided the most favorable balance and reached a compressive strength of approximately 20 MPa, close to that of the M40 reference mixture. The lower performance of the C:3–8 and C:3–8/8–15 mixtures can reasonably be associated with differences in particle packing and the intrinsic mechanical characteristics of the CDR aggregate. Consequently, the 8–15 mm CDR fraction was selected for the subsequent stages of the study, particularly for the manufacture and characterization of the solid bricks. This selection provides a rational basis for developing a practical cement-based building material that combines 40% dune sand with locally available crushed desert rose aggregate, thereby contributing to the valorization of regional mineral resources and the development of more sustainable construction materials.

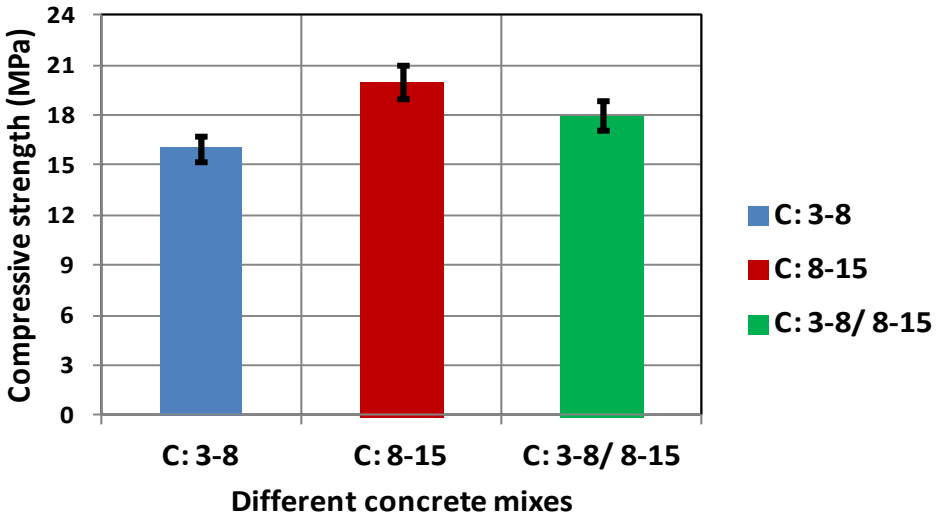


Fig. 12. Compressive strength of different concrete mixes

4.2 Physical Properties

4.2.1 Water Absorption Through Total Immersion

Figure 13 indicates that the grain size of the crushed desert rose aggregate (CDR) exerts a significant influence on the water-accessible porosity of the concrete matrix. The variation in water

absorption as a function of aggregate size can be attributed to key morphological, microstructural, and physical mechanisms.

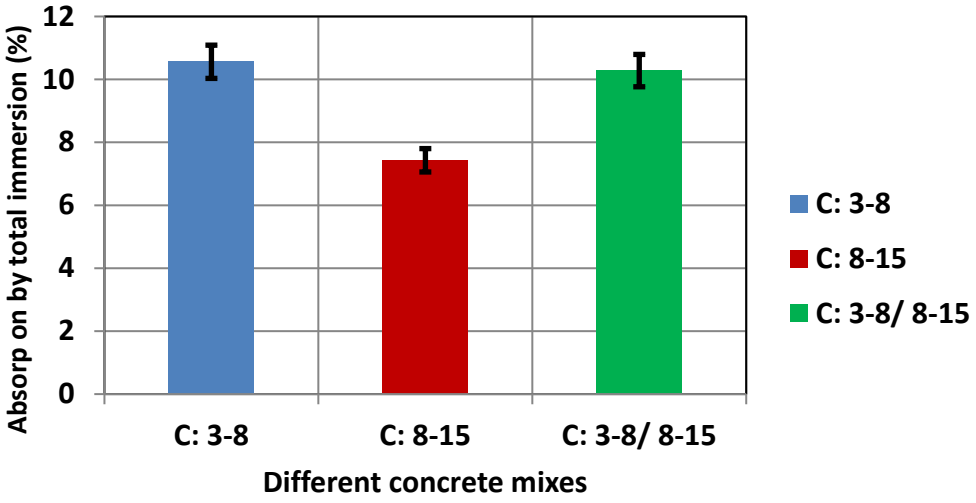


Fig. 13. Water absorption by total immersion

Specific surface area and porosity: crushed desert rose is a naturally gypsum-based, porous, and friable material. Processing it into a finer fraction (3-8mm) substantially increases its overall specific surface area within the concrete matrix. This higher surface area expands the interface exposed to water and increases the total volume of the Interfacial Transition Zone (ITZ)—a region inherently characterized by higher capillary porosity and permeability. Packing Density of the 8–15 mm Fraction: Conversely, utilizing the coarser fraction (8-15mm) lowers the aggregate's specific surface area. This allows for a more uniform and continuous coating by the cement paste, which reduces capillary network continuity and hinders water penetration, resulting in a denser matrix (7.42 %). Dominance of Fines in the Bimodal Mix: In the combined mix (3-8 / 8-15mm), water absorption remains elevated (10.28%). Although combining two fractions theoretically enhances skeletal packing density, the presence of the fine fraction (3-8 mm) reintroduces a high specific surface area and dominant capillary porosity, effectively masking any beneficial effect of the coarser aggregates.

4.2.2 Water Capillary Absorption (WCA)

- Water absorption kinetics and capacity analysis

Figure 14 shows the water absorption kinetics over a 72-hour immersion period for three different concrete formulations (C: 3-8, C: 8-15, and the combined formulation C: 3-8/8-15). Overall, all formulations exhibit typical two-phase absorption behavior: a sharp initial mass increase during the first 8 hours (capillary absorption phase), followed by a gradual slowdown to asymptotic stabilization between 24 and 72 hours (saturation equilibrium phase), as reported in similar porous matrices studied by (Nan et al., 2025) [48]. Although sample C: 8-15 has the highest initial dry mass (2112 g) and the highest total mass at saturation (2210 g), it displays the lowest relative water absorption capacity, with a gain of only about 98 g (approximately 4.64%) (Figure 15). This suggests a denser structure with reduced open capillary porosity. Conversely, the C:3-8 fine monogranular aggregate formulation absorbs approximately 160 g (≈ 7.98%) of water (Figure 15). The binary aggregate mixture C:3-8/8-15 exhibits the highest water absorption gain, increasing from an initial dry mass of 1950 g to 2128 g, a gain of 178 g (≈ 9.13%) (Figure15). This increased water absorption capacity of the mixture can be attributed to greater intergranular capillary porosity or a larger microvoid network, which facilitates greater capillary suction during the initial immersion phase, [49, 50]. These results are entirely consistent with those already found for absorption by total immersion (Figure 13). The higher relative absorption recorded for the blended aggregate formulation (C: 3-8 / 8-15) can be attributed to the altered inter-granular porosity and capillary interconnectivity, which enhances initial water uptake [49, 50].

- Capillary sorptivity analysis

Figure 16 illustrates the sorptivity coefficient (S) of the three concrete mixes: C:3-8, C:8-15, and C:3-8/8-15. The sorptivity coefficient, expressed in ($g/cm^2.h^{0,5}$) provides a direct evaluation of the capillary suction rate and the interconnectivity of the pore network within the matrix (Nan et al., 2025). Among the three formulations, the coarse aggregate concrete (C: 8-15) exhibits the lowest sorptivity value (0.113 $g/cm^2.h^{0,5}$), indicating a greater resistance to water transport. This can be attributed to the lower specific surface area of the coarse CDR fraction, which reduces the total volume of interfacial transition zones (ITZ) and limits capillary action. In contrast, reducing the CDR aggregate size to C: 3-8 leads to a significant increase in sorptivity 0.190 $g/cm^2.h^{0,5}$. The highest sorptivity coefficient is recorded for the binary aggregate blend (C: 3-8 / 8-15), peaking at 0.210 $g/cm^2.h^{0,5}$, representing an 85% increase relative to the C: 8-15 mix. This enhanced capillary absorption in the blended CDR concrete is likely caused by the combined effect of the micro-porous nature of crushed sand rose particles and the high fineness of the dune sand (40%). The combination of binary CDR fractions with fine dune sand alters the granular packing, resulting in a higher density of interconnected capillary pores and an expanded ITZ surface area around the porous crushed sand rose grains [49, 50].

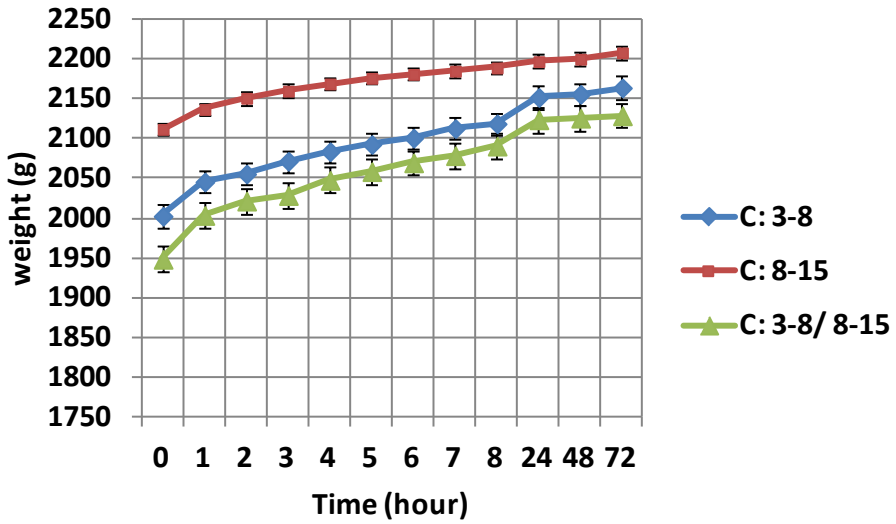


Fig. 14. Mass gain of the different concrete specimens during the capillary water absorption test

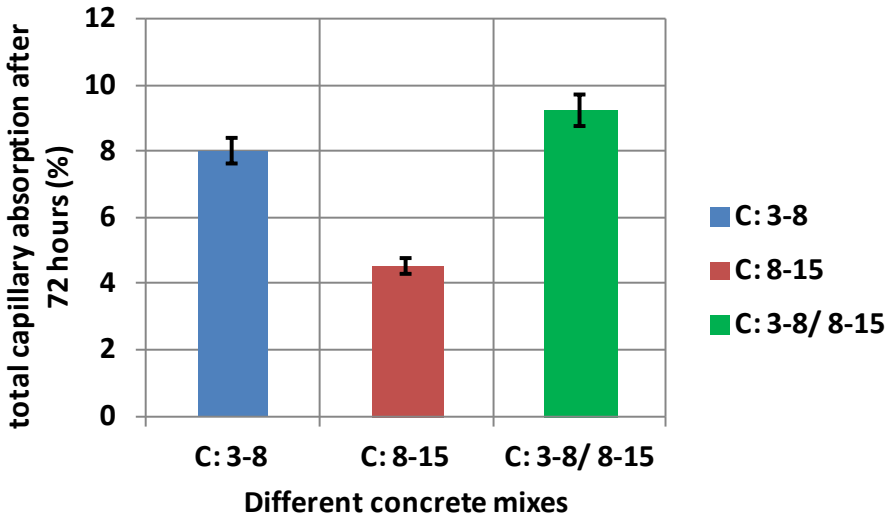


Fig. 15. Total capillary water absorption after 72 h

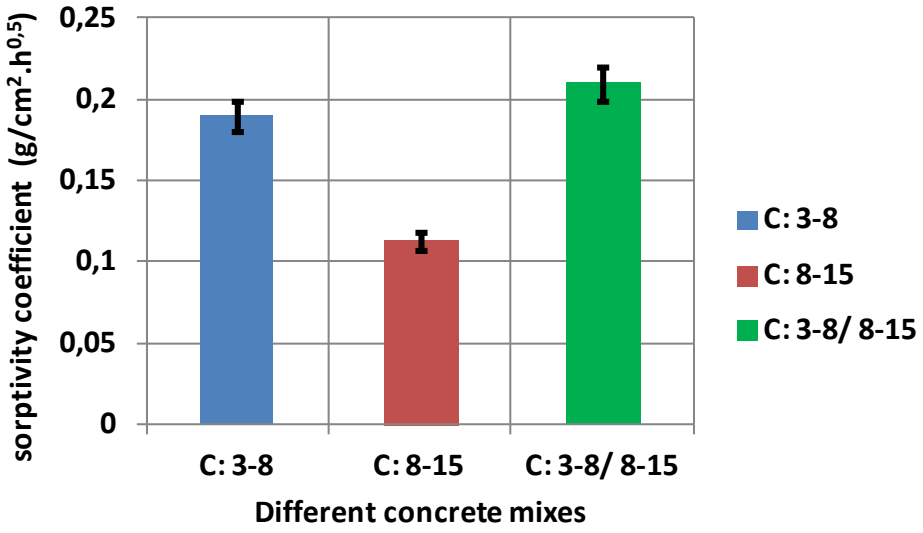


Fig. 16. Sorptivity coefficients of the investigated concrete mixtures

4.2.3 Ultrasonic Pulse Velocity (UPV)

Figure 17 presents the Ultrasonic Pulse Velocity (UPV) values for the three studied concrete formulations. The fine aggregate formulation (C: 3-8) recorded the highest velocity at approximately 3890 m/s. According to standard quality classifications (IS 13311 and BS 1881), values ranging between 3500 m/s and 4500m/s indicate a "Good" quality concrete matrix. This elevated velocity indicates an optimized packing density where finer Crushed desert rose (CDR) particles, combined with the ultra-fine dune sand fraction (40%), effectively fill internal micro-voids, creating a continuous and compact path for ultrasonic wave propagation [50]. The binary aggregate mixture (C: 3-8 / 8-15) exhibits a slightly lower pulse velocity (3720 m/s), remaining within the same structural quality category.

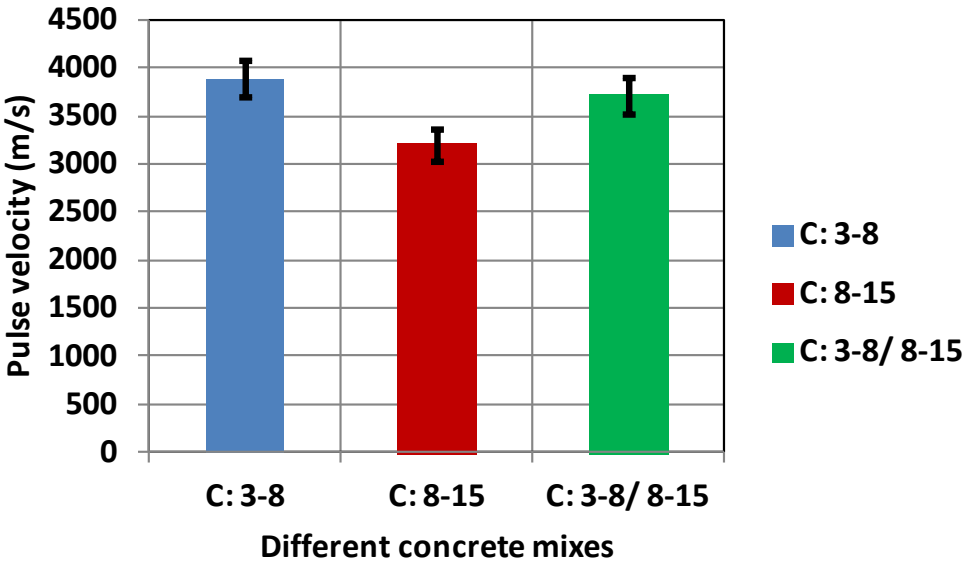


Fig. 17. Ultrasonic pulse velocity of the investigated concrete mixtures

In contrast, the coarse aggregate concrete (C: 8-15) shows a noticeable decrease in wave velocity, dropping to approximately 3210 m/s (classified as "Medium" quality). This reduction in velocity for the C: 8-15 mix can be attributed to the porous intrinsic structure of larger crushed sand rose aggregates, combined with a higher proportion of coarse void networks and weaker Interfacial Transition Zones (ITZ). Larger aggregate sizes create tortuous paths and internal air-void interfaces that attenuate and slow down the propagation of ultrasonic waves through the composite material [48].

4.3 Thermal Characterization

4.3.1 Thermal Insulation and Transient Temperature Response

Figures 18 and 19 illustrate the internal (Tint) and external (Text) surface temperature evolution for the three composite brick formulations during a 150-minute heating phase followed by a cooling period, under a stable ambient temperature (Tamb ≈ 28 - 30°C). These results can be analyzed as follows:

- Internal Surface Temperature (Tint):

During the heating phase (0-150min), all brick specimens showed a continuous rise in internal face temperature due to direct conductive heat transfer from the heating plate. At the end of the heating cycle (150min), the coarse aggregate formulation (C: 8-15) recorded the highest internal temperature, reaching approximately 65°C, followed by the binary blend C: 3-8 / 8-15 (62°C). In contrast, the fine aggregate formulation (C: 3-8) demonstrated a significantly lower thermal accumulation, peaking at only 55°C; a reduction of 10°C relative to the coarse mix [51]. Upon shutting off the heating source (150-300 min), a rapid thermal dissipation phase was observed across all samples, gradually converging back toward Tamb.

- External surface temperature (Text) and thermal resistance:

The outer surface temperature profiles (Text) further highlight the thermal insulating performance of the composite bricks (Figure 19). A distinct thermal lag and temperature attenuation were observed, as maximum (Text) values remained below 52°C across all samples. Consistently, the C: 3-8 brick exhibited the lowest outer surface temperatures throughout the heating period, peaking at ≈ 46°C at 150 min.

- Physical Interpretation:

The superior thermal insulation capability of the C: 3-8 composite brick can be attributed to its optimized microstructural packing when combined with 40% fine dune sand (DS) and crushed sand rose aggregates (CDR). Finer CDR aggregate sizing promotes a higher distribution of non-connected intra-particle micro-pores and interfacial air voids, which significantly restricts lattice thermal conductivity. Conversely, the coarser C: 8-15 aggregate matrix creates larger conductive solid bridges across the aggregate framework, facilitating faster heat propagation through the brick thickness [50].

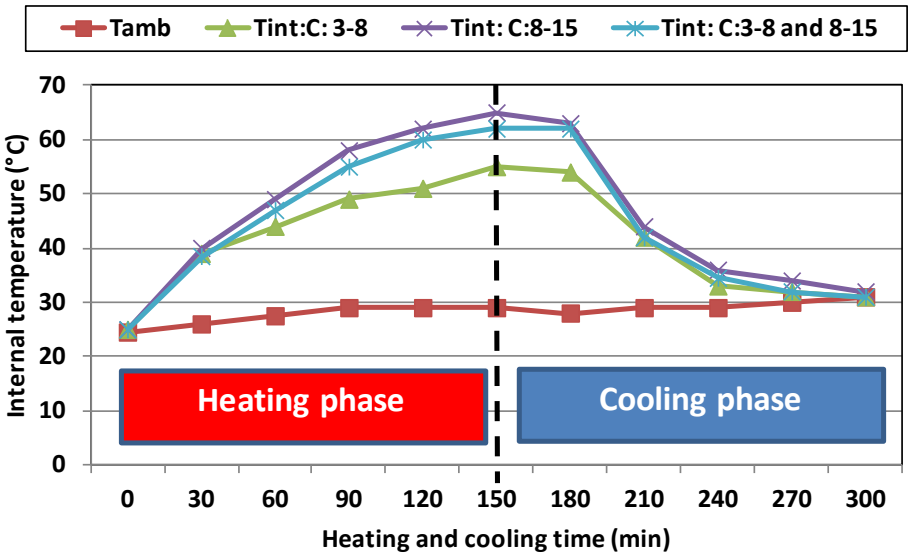


Fig. 18. Internal temperature variation (Tint) of crushed desert rose composite bricks during transient thermal testing

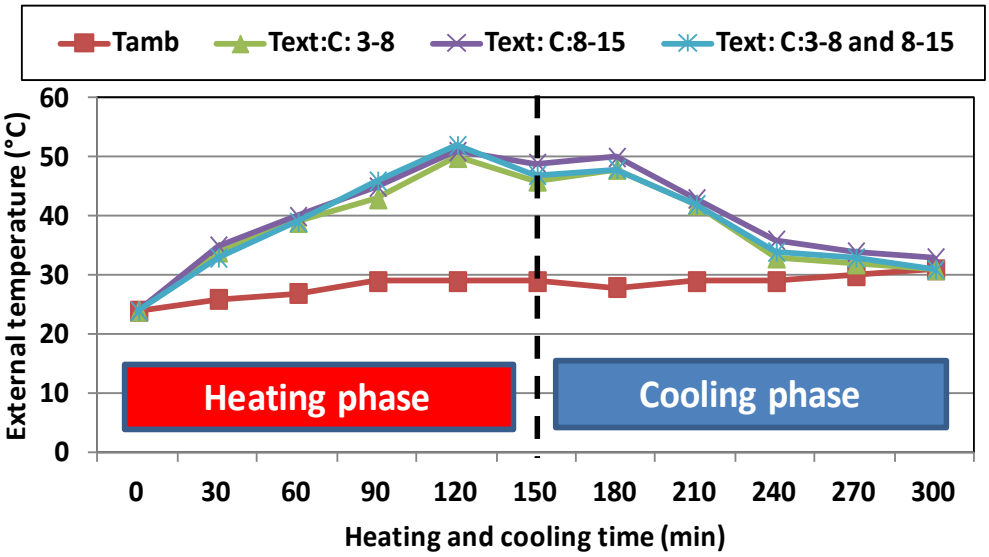


Fig. 19. External temperature variation (Text) of crushed desert rose composite bricks during transient thermal testing

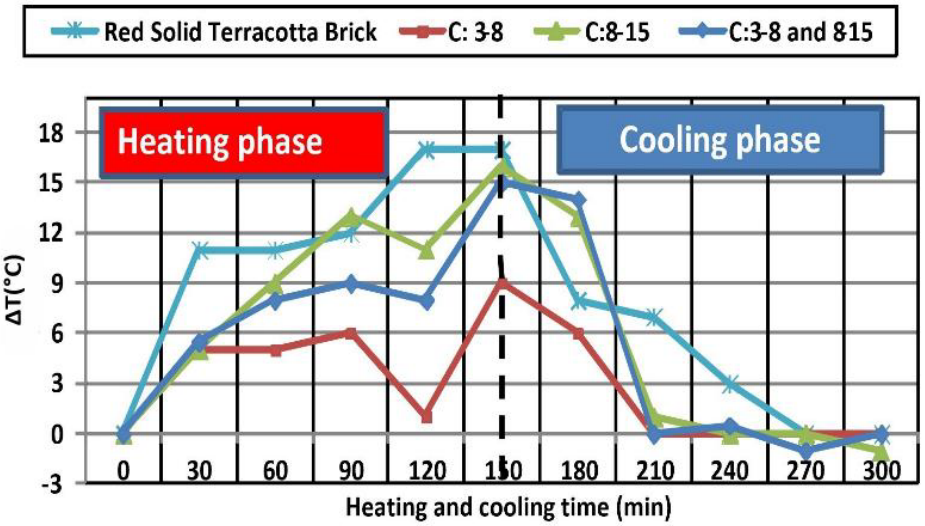


Fig. 20. Thermal gradient profiles of local CDR composite bricks and conventional terracotta brick during thermal exposure

4.3.2 Thermal Gradient (ΔT) Analysis & Comparative Justification

- Thermal gradient evolution (ΔT = Tint- Text) and comparative evaluation

Figure 20 depicts the temperature difference (ΔT) between the inner heated surface (Tint) and the outer unheated surface (Text) for the three eco-friendly composite bricks compared to a conventional Red Solid Terracotta Brick. The thermal gradient (ΔT) serves as a crucial indicator of heat propagation resistance and transient thermal damping across the masonry unit thickness [52].

During the heating stage (0-150min), the reference terracotta brick reached the highest temperature gradient, peaking at ΔT=17°C. This elevated differential reflects significant heat entrapment at the exposed face combined with a delayed thermal transfer to the opposite side. Among the developed eco-composite bricks, the coarse formulation (C: 8-15) and the binary formulation (C: 3-8 / 8-15) displayed strong thermal resistance, reaching peak gradients of 16°C and 15 °C at 150 min, respectively—values remarkably close to commercial terracotta brick. Conversely, the fine aggregate brick (C: 3-8) maintained a lower and more uniform thermal gradient throughout the heating phase (ΔT≈5-6°C up to 90min, peaking at 9°C at 150 min).

- Scientific justification & performance advantage:

The comparative performance demonstrates that substituting traditional clay bricks with composite units formulated from local crushed sand rose aggregates (CDR) and 40 % dune sand (DS) provides equivalent—and in specific cases, superior—thermal regulation:

- Thermal Damping and Insulation Equivalency: Formulations C: 8-15 and C: 3-8 / 8-15 match the thermal barrier capabilities of commercial red solid clay bricks, validating their structural viability for energy-efficient building envelopes in arid climates [4, 20, 51].
- Microstructural Heat Dispersal: The incorporation of porous CDR particles paired with fine dune sand optimizes the internal pore tortuosity. This restricts rapid heat conduction while maintaining lower surface thermal stress (ΔT), thereby minimizing the risk of thermally induced micro-cracking during severe ambient heating cycles.

5. Conclusions

This study demonstrates the technical feasibility and environmental viability of formulating sustainable composite bricks utilizing crushed desert rose aggregates (CDR) and Saharan dune sand (DS). Beyond offering an innovative material solution, this approach effectively valorizes abundant local desert resources, thereby advancing sustainable construction while safeguarding the architectural and historical heritage of the region. Based on the comprehensive experimental evaluation of mechanical, physical, and thermal properties, the following core conclusions are drawn:

- Optimized Mechanical Performance: Partial substitution of alluvial sand with dune sand (10% to 40%) significantly enhances granular packing density. Peak flexural strength was achieved at a 10% substitution ratio (M10), yielding a 43% increase in flexural strength and a 10% improvement in compressive strength compared to the control mortar. Flexural strength remained superior up to a 40% replacement level (+21%), which justified selecting a 40% incorporation rate to maximize the valorization of local dune sand.
- Structural Concrete Formulations: All three concrete formulations prepared with dune sand (DS) and crushed sand rose aggregates (CDR) exhibited highly acceptable compressive strengths exceeding 16MPa. Notably, the formulation C: 8-15 demonstrated the highest performance, achieving a maximum compressive strength of 20 MPa.
- Controlled Transport Properties: Non-destructive Ultrasonic Pulse Velocity (UPV) analysis confirmed that finer aggregate fractions (C: 3-8) produce a dense and homogeneous structural matrix (3890 m/s, classified as "Good" quality concrete). Additionally, aggregate grading directly regulates capillary sorptivity, with the coarse fraction (C: 8-15) offering the highest resistance to water ingress (0.113 g/cm2.h0,5).
- Superior Thermal Insulation for Hot Climates: Transient thermal testing highlights the exceptional thermal barrier capabilities of the developed CDR-DS composite bricks. The C: 3-8 formulation exhibited remarkable thermal insulation, reducing internal surface temperatures by up to 10°C relative to coarser mixes. Crucially, the developed eco-composite bricks demonstrated thermal damping profiles (ΔT=Tint-Text up to 16°C) that rival conventional commercial red solid terracotta bricks.

In conclusion, valorizing local crushed sand rose aggregates and Saharan dune sand offers a double advantage: it provides an eco-friendly alternative to scarce natural aggregates while producing energy-efficient masonry units specifically suited for reducing cooling loads in hot and arid environments.

Although this study successfully demonstrates the potential of developing an innovative cementitious composite material utilizing Saharan dune sand (DS) and crushed sand rose aggregates (CDR), several limitations should be acknowledged:

- Laboratory-Scale Evaluation: The experimental testing was conducted under controlled laboratory conditions, which may not fully capture the complex, transient thermo-hygrometric behavior of the material when exposed to real-world operational environments.

- Scope of Formulations: The investigation focused on specific particle size distributions and combinations, primarily evaluating two main aggregate fractions (C: 3-8 and C: 8-15) alongside their binary mix (C: 3-8 / 8-15), leaving alternative mix proportions unexplored.
- Environmental & Life-Cycle Assessment: The broader environmental impact, embodied energy, and life-cycle assessment (LCA) of the composite units were not quantitatively evaluated in this phase.

To facilitate the practical deployment of these composite bricks, several key aspects warrant further investigation. Given the inherent water absorption of gypsum-rich aggregates, future work should primarily focus on evaluating long-term cement–gypsum compatibility and overall durability. Specifically, performance under wet/dry cycling, elevated-temperature exposure, and long-term dimensional and mechanical stability should be thoroughly assessed

Acknowledgements

The authors gratefully acknowledge the Directorate General for Scientific Research and Technological Development (DGRSDT) for its support. They also sincerely thank the staff of the Unit for the Development of Renewable Energy in Arid Areas (UDERZA) and the Laboratory for the Exploitation and Valorization of Saharan Energy Resources (LEVRES), Faculty of Exact Sciences, University of El Oued, for their valuable assistance.

References

[1]. Algérie Presse Service (APS). Website of Algérie Presse Service (APS) [Internet]. 2026 [cited 2026 Jul 13]. Available from: https://www.aps.dz/fr

[2]. World Bank. Algeria Overview [Internet]. 2024. Available from: https://www.worldbank.org/en/country/algeria/overview

[3]. Asfaw NT, Absi R, Labouda BA, El Abbassi I. Assessment of the thermal and mechanical properties of bio-based composite materials for thermal insulation: A review. Journal of Building Engineering. 2024;98:111120. https://doi.org/10.1016/j.jobe.2024.110605

[4]. Lu Z, Hauschild M, Ottosen LM, Ambaye TG, Zerbino P, Aloini D. Climate mitigation potential of biobased insulation materials: A comprehensive review and categorization. Journal of Cleaner Production. 2024;470:143356. https://doi.org/10.1016/j.jclepro.2024.143356

[5]. Zhang Y, Sattar S, Cook D, Johnson K, Fung J. Systematic Review of Embodied Carbon Assessment and Reduction in Building Life Cycles. National Institute of Standards and Technology (NIST), Special Publication 1324; 2024. https://doi.org/10.6028/NIST.SP.1324

[6]. Pawłosik D, Cebrat K, Brzezicki M. Exploring advancements in bio-based composites for thermal insulation: A systematic review. Sustainability. 2025;17(3):1143. https://doi.org/10.3390/su17031143

[7]. Ye F, Wei H, Xiao Y, Berardi U, Quaranta G, Demartino C. Bio-based insulation materials in sustainable constructions: A review of environmental, thermal and acoustic insulation, durability, and mechanical performances. Renewable and Sustainable Energy Reviews. 2025;223:115872. https://doi.org/10.1016/j.rser.2025.115872

[8]. Lasbet C, Bederina M, Makhloufi Z, Djoudi A. Sustainable and eco-friendly lightweight sand concrete reinforced with natural Alfa fibers and wood shavings: mechanical, thermal and acoustic characterization. Journal of Adhesion Science and Technology. 2026:1-37. https://doi.org/10.1080/01694243.2026.2668556

[9]. Yousaf A, Khan SA, Koç M. Multi-scale characterization of acacia gum as an alternative plant-based biopolymer binder for CO2 sequestering earthen soil composites. Emergent Mater. 2026;9:55. https://doi.org/10.1007/s42247-026-01355-1

[10]. Yousaf A, Khan SA, Koç M. Proof-of-concept design, characterization, and life cycle assessment of recycled PET-sand composite bricks via solvent-based dissolution. Construction and Building Materials. 2025;491:142612. https://doi.org/10.1016/j.conbuildmat.2025.142612

[11]. Azil C, Djebri B, Fratini F, Misseri G, Rovero L. Desert Rose Stone Constructions Covered with Domes in the Souf Region (Algeria). International Journal of Architectural Heritage. 2020. https://doi.org/10.1080/15583058.2020.1813353

[12]. Rachedi M, Kriker A. Investigation of the mechanical and thermal characteristics of an eco-insulating material made of plaster and date palm fibers. SSP - Journal of Civil Engineering. 2021;16(2). https://doi.org/10.2478/sspjce-2021-0016

[13]. Rachedi M. Contribution à l'étude du comportement thermique du plâtre renforcé par des fibres de palmier dattier [doctoral thesis]. Ouargla, Algeria: University of Ouargla; 2024.

[14]. Yousaf A, Rashid AA, Koç M. Additive manufacturing for vernacular architecture using local earthen soil and bio-waste materials. Engineering Structures. 2025;344:121321. https://doi.org/10.1016/j.engstruct.2025.121321
[15]. Yousaf A, Khan SA, Koç M. 3DP for sustainable built environment - Synthesis and thermomechanical characterization of composite materials based on local soil and date palm fiber waste. Journal of Cleaner Production. 2024;481:144050. https://doi.org/10.1016/j.jclepro.2024.144050
[16]. Rachedi M, Kriker A. Thermal properties of plaster reinforced with date palm fibers. Civil and Environmental Engineering. 2020;16(2):259-266. https://doi.org/10.2478/cee-2020-0025
[17]. Braiek A, Karkri M, Adili A, Ibos L, BenNasrallah S. Estimation of the thermo-physical properties of date palm fibers/gypsum composite for use as insulating materials in building. Energy and Buildings. 2017;140:268-279. https://doi.org/10.1016/j.enbuild.2017.02.001
[18]. Khrissi Y, Tilioua A, Laaroussi N. Thermal Characterization of a New Bio-Composite Building Material based on Gypsum and Date Palm Fiber. Materials Research Proceedings. 2024;40:55-63. https://doi.org/10.21741/9781644903117-6
[19]. Azil C, Vicario M. Learning from the past: old and new ksour in the M'Zab Valley (Algeria). Restauro Archeologico. 2023;30(1). https://doi.org/10.36253/rar-14286
[20]. Lechheb M, Chrachmy M, Ben Baaziz M, El Boukili G, Ouallal H, Azdouz M, et al. Mechanical and thermal properties of goulmima's earth bricks. In: Mediterranean Architectural Heritage. Materials Research Proceedings; 2024. https://doi.org/10.21741/9781644903117-21
[21]. Hafsi F, Kriker A, Abani S. Contribution study to the thermal insulation of the builders in the desert regions of exploiting gypsum fiber reinforced palm. In: Technologies and materials for renewable energy, environment and sustainability: TMREES16-Cnam. AIP Conference Proceedings. 2017;1814(1):020029. https://doi.org/10.1063/1.4976248
[22]. Mekhermeche A, Kriker A, Dahmani S. Contribution to the study of thermal properties of clay bricks reinforced by date palm fiber. In: Technologies and materials for renewable energy, environment and sustainability: TMREES; 2016. https://doi.org/10.1063/1.4959400
[23]. Kriker A, Abani S, Bouziane M, Hafsi F. Date Palm Fiber Composites in Hot-Dry Construction and Building. In: Date Palm Fiber Composites. 2020. https://doi.org/10.1007/978-981-15-9339-0_12
[24]. Logbi A, Djedid T, Boumaaza M, Belaadi A, Alshaikh IM, Far A, et al. Characterizing thermally and physico-mechanically an eco-friendly insulating brick made from gypsum and crushed sand rose stone using RSM and ANN. Case Studies in Construction Materials. 2025;22:e05673. https://doi.org/10.1016/j.cscm.2025.e05673
[25]. Logbi A, Mani M, Choungara T, Kriker A. Comparative study of the effect of crushed dune sand and limestone fillers on mortar properties in aggressive environment. World Journal of Engineering. 2023;20(1):85-92. https://doi.org/10.1108/WJE-09-2020-0437
[26]. Alahmad FA, El Maaddawy T, Abu-Jdayil B. Performance evaluation of date-pit-reinforced unsaturated-polyester-dune-sand mortars. Construction and Building Materials. 2025;462:139965. https://doi.org/10.1016/j.conbuildmat.2025.139965
[27]. Beldjilali S, Bougara A, Aguiar J, Bouhamou N, Dabbebi R. Properties of a new material based on a gypsum matrix incorporating waste brick. Construction and Building Materials. 2020;259:120416. https://doi.org/10.1016/j.conbuildmat.2020.120416
[28]. Jawad A, Ali MA, Deifalla AF, et al. Concrete made with dune sand: Overview of fresh, mechanical and durability properties. Materials. 2022;15(17):6152. https://doi.org/10.3390/ma15176152
[29]. Zerig T, Aidoud A, Belachia M, Djedid T, Abbas M. Combined sand eco-mortar reinforced with polyethylene terephthalate: behavior and optimization using RSM method. Constr Build Mater. 2023;404:133160. https://doi.org/10.1016/j.conbuildmat.2023.133160
[30]. Zerig T, Belachia M, Aidoud A, Meftah N, Djedid T, Abbas M. Statistical analysis using the RSM approach of the physical behavior of green polymerized eco-mortar. J Clean Prod. 2024;450:141858. https://doi.org/10.1016/j.jclepro.2024.141858
[31]. Djedid T, Mani M, Guettala A, Hima A. Analysis of workability, mechanical strength and durability by the FT-IR method of concrete based on silica-limestone sand preserved in aggressive environments. Frattura ed Integrita Strutturale. 2022;15:566-579. https://doi.org/10.3221/IGF-ESIS.59.37
[32]. Djedid T, Mani M, Ouakouak A, Guettala A. Effect of varying silica-limestone sand fines on the physicalmechanical performance of concrete. Frattura ed Integrita Strutturale. 2022;16:580-591. https://doi.org/10.3221/IGF-ESIS.59.38
[33]. Hafhouf I, Karouche A, Benalia A, Roubeche C, Hitani I, Duc M, et al. Assessment of ground dune sand (GDS) in the production of air lime mortars for historic buildings restoration. Construction and Building Materials. 2025;481. https://doi.org/10.1016/j.conbuildmat.2025.141604
[34]. Dias S, Almeida J, Tadeu A, de Brito J. Alternative concrete aggregates: Review of physical and mechanical properties and successful applications. Cement and Concrete Composites. 2024;152:105663. https://doi.org/10.1016/j.cemconcomp.2024.105663

[35]. Akhtar MN, Bani-Hani KA, Malkawi DAH, Albatayneh O. Suitability of sustainable sand for concrete manufacturing: A complete review of recycled and desert sand substitution. Results in Engineering. 2024;23:102478. https://doi.org/10.1016/j.rineng.2024.102478
[36]. Soleilhavoup F. Microformes d'accumulation et d'ablation sur les surfaces désertiques du Sahara. Géomorphologie : relief, processus, environnement. 2013;17(2):173-186. https://doi.org/10.4000/geomorphologie.9376
[37]. Meftah N, Hani A. Characterization of Algerian dune sand as a source to metallurgical-grade silicon production. Materials Today: Proceedings. 2022;51:2105-2108. https://doi.org/10.1016/j.matpr.2021.12.366
[38]. Daheur EG, Goual I, Taibi S, Mitiche-Kettab R. Effect of dune sand incorporation on the physical and mechanical behaviour of tuff: Experimental investigation. Geotechnical and Geological Engineering. 2018;37(3):1687-1701. https://doi.org/10.1007/s10706-018-0715-4
[39]. Zhang M, Zhu X, Shi J, Liu B, He Z, Liang C. Utilization of desert sand in the production of sustainable cement-based materials: A critical review. Construction and Building Materials. 2022;348:128780. https://doi.org/10.1016/j.conbuildmat.2022.127014
[40]. Mani M, Kriker A, Belferrag A. Compressive strength of dune sand reinforced concrete. AIP Conference Proceedings. 2017;1814(1):020023. https://doi.org/10.1063/1.4976242
[41]. NF EN 933-1 standard. Tests for geometrical properties of aggregates. Part 1 : determination of particle size distribution. Sieving method; 2012.
[42]. NBN B 15-215 Standard. Tests on hardened concrete - Water absorption by immersion; 2018.
[43]. EN 1015-18. Determination of water absorption coefficient due to capillary action of hardened mortar, 3; 2002.
[44]. BS EN 12504-4 standard. Determination of ultrasonic pulse velocity; 2004.
[45]. EN 196-1 standard. Methods of testing cement - Part 1: Determination of strength; 2016.
[46]. Hamada HM, Abed F, Al-Sadoon ZA, Elnassar Z, Hassan A. The use of treated desert sand in sustainable concrete: A mechanical and microstructure study. Journal of Building Engineering. 2023;79:107843. https://doi.org/10.1016/j.jobe.2023.107843
[47]. Ukpata JO, Ewa DE, Success NG, et al. Effects of aggregate sizes on the performance of laterized concrete. Scientific Reports. 2024;14:448. https://doi.org/10.1038/s41598-023-50998-1
[48]. Nan F, Zhao X, Zhang Y, Liu C. Capillary water absorption characteristics of steel fiber-reinforced concrete. Buildings. 2025;15(9):1542. https://doi.org/10.3390/buildings15091542
[49]. Ding Y, She A, Yao W. Investigation of water absorption behavior of recycled aggregates and its effect on concrete strength. Materials. 2023;16(13):4505. https://doi.org/10.3390/ma16134505
[50]. Wang Y, Zhang X, Liu Y. Factors influencing the capillary water absorption characteristics of concrete and their relationship to pore structure. Applied Sciences. 2022;12(4):2211. https://doi.org/10.3390/app12042211
[51]. El-Emam M, Al-Tamimi A. Strength and Deformation Characteristics of Dune Sand Earth Blocks Reinforced with Natural and Polymeric Fibers. Sustainability. 2022;14(8):4850. https://doi.org/10.3390/su14084850
[52]. Hamadou-Ali M, Mezreb K, Benazzouk A, Ben Hamed H. Development of cellular construction material-based flax shives: Physico-mechanical and thermal characterization. MATEC Web of Conferences. 2024;394:02001. https://doi.org/10.1051/matecconf/202439402001